HHS Public Access

Author manuscript

Chem Phys Lett. Author manuscript; available in PMC 2019 August 16.

Published in final edited form as:

Chem Phys Lett. 2018 August 16; 706: 741–752. doi:10.1016/j.cplett.2018.06.019.

Single Quantum Dot Tracking Illuminates Neuroscience at the Nanoscale

Oleg Kovtun[1,5], **Ian D. Tomlinson**[1,5], **Danielle M. Bailey**[1,2,5], **Lucas B. Thal**[1,5,6], **Emily J. Ross**[7], **Lauren Harris**[6], **Michael P. Frankland**[1], **Riley S. Ferguson**[1], **Zachary Glaser**[1], **Jonathan Greer IV**[1], and **Sandra J. Rosenthal**[1,2,3,4,5,6,*]

[1]Departments of Chemistry, Chemical Biology, Vanderbilt University

[2]Departments of Pharmacology, Chemical Biology, Vanderbilt University

[3]Departments of Chemical and Biomolecular Engineering, Chemical Biology, Vanderbilt University

[4]Departments of Physics and Astronomy, Chemical Biology, Vanderbilt University

[5]Departments of Vanderbilt Institute of Nanoscale Science and Engineering

[6]Departments of Vanderbilt Institute of Chemical Biology, Vanderbilt University, Nashville, TN

[7]Departments of Hudson Alpha Institute for Biotechnology, Huntsville, AL.

Abstract

The use of nanometer-sized semiconductor crystals, known as quantum dots, allows us to directly observe individual biomolecular transactions through a fluorescence microscope. Here, we review the evolution of single quantum dot tracking over the past two decades, highlight key biophysical discoveries facilitated by quantum dots, briefly discuss biochemical and optical implementation strategies for a single quantum dot tracking experiment, and report recent accomplishments of our group at the interface of molecular neuroscience and nanoscience.

Introduction.

Technological innovation in the field of fluorescence microscopy over the past two decades has elevated our ability to observe single molecules at work in living cells. A fluorescence microscope is now the backbone of modern molecular, cellular, and developmental biology labs, driving the discovery of molecular mechanisms that underlie fundamental biological processes. Single particle tracking (SPT) has emerged as a particularly powerful fluorescence microscopy technique, since it allows researchers to directly record how individual molecules traffic, interact, self-assemble, and undergo conformational changes at millisecond temporal and nanometer spatial resolution. One of the toughest early hurdles in SPT was the limited photon budget of a single molecule – an organic dye or a fluorescent protein only emit 10^5-10^6 photons before they enter a permanent nonemissive dark state, severely reducing the localization accuracy and trajectory duration [1–3]. Such rapid

*corresponding author: sandra.j.rosenthal@vanderbilt.edu.

Supporting Information. Materials and methods for previously unpublished findings in Section 3.3 and Section 3.4 are provided.

photobleaching of conventional fluorescent probes was overcome with the use of quantum dots (QDs), one of the first nanotechnologies integrated with biology [4,5]. QDs are nanometer-sized semiconductor crystals that are characterized by relatively small size (2–10 nm) and size-tunable, narrow, Gaussian emission spectra. QDs feature broad absorption spectra, which readily enable multiplexed experiments with a single excitation source. Their high brightness is a product of high quantum yields, high molar extinction coefficients, and excellent photostability [1–5]. Although QDs were introduced to the field of biology in 1998, it took several years to optimize their colloidal stability in aqueous solutions and biocompatibility with live cell imaging. In 2003, QDs were for the first time implemented in a SPT experiment, wherein Dahan *et al.* imaged the rapid diffusion of QD-tagged endogenous glycine receptors in and out of FM4–64 dye-labeled synaptic boutons in the rat spinal cord cultures [6]. The ensuing QD-based discovery and characterization of the protein motion in living cells led to the following important discoveries: (i) the plasma membrane, in contrast to the “fluid mosaic” model, is compartmentalized into dynamic, multitiered nanodomains stabilized and organized by cholesterol, actin cytoskeleton, and various scaffolding proteins [3,7]; (ii) the kinetic trapping by specialized nanodomains is an essential feature of the spatial organization and activity fine-tuning of transmembrane proteins [7,8]; (iii) transmembrane proteins undergo transient homo- and heterooligomerization in response to stimuli [7]; and (iv) posttranslational modifications regulate neuronal protein synaptic recruitment via changes in lateral protein motion [8]. Moreover, several groups reported evidence of non-ergodic behavior of QD-tagged membrane proteins, breaking with the ergodic hypothesis, which postulates that tracking a single representative species over a long time period provides the same information about an ensemble of identical species as observing the ensemble itself [18]. Such time- and space-dependent variation in diffusivity of de-facto biochemically identical species in SPT studies is likely a manifestation of the conformational state flux, covalent protein modifications, ligand binding events, and transient interactions with the local microenvironment. In the same span of time, the following QD SPT developmental milestones were achieved – multiplexed SPT of up to 8 spectrally distinct QD species [9], QD SPT in living rat brain slices [10,11], QD SPT in 3D by means of an astigmatic lens [12], an engineered double helix point spread function [13], or a multifocal plane setup [14], and high-speed SPT at acquisition rates > 1 kHz [15] (Table 1). In the subsequent sections of this article, we will provide a brief overview of important QD probe design considerations, describe a basic framework for optical QD SPT implementation to obtain highest quality data, and report key biological findings obtained using QD SPT in our group. Then, we will discuss the existing QD drawbacks, compare and contrast QD SPT with competing single-molecule imaging techniques, and offer possible solutions to the challenges that QD-based SPT is currently facing.

2.1. QD Probe Generation and Target Specificity Assessment.

Arguably, specific recognition of the target biomolecule by any SPT probe is the most important property. Although fluorescent proteins offer perfect specificity due to the genetic fusion to the target protein, they are incompatible with endogenously expressed species, and it is often difficult to distinguish between membrane-limited and intracellular diffusive events. On the other hand, nonspecific binding to the plasma membrane and the coverslip is

a commonly encountered issue when using externally applied probes such as organic dyes and QDs [19]. In fact, the more hydrophobic organic dyes are notorious for such nonspecific binding, potentially introducing two types of artifacts into SPT experiments: (i) nonspecific dye adhesion to the substrate on which cells are cultured might result in a non-trivial increase in the immobile probe population and (ii) probes nonspecifically bound to the plasma membrane appear to exhibit pure Brownian motion and might diffuse at rates higher than the target biomolecule [19,20]. In contrast, a commercially available QD architecture (Thermo Fisher Scientific) features a polyethylene glycol layer that effectively minimizes QD nonspecific binding to both the cell membrane and glass [21], though it is still recommended that QD nonspecific binding is assessed on a case-by-case basis, with the necessary blocking reagents (serum, casein, nonfat dry milk) used to reduce the residual nonspecific binding.

Several approaches are available to impart the QD with target specificity [2,3,22]. The most popular strategy relies on the use of primary antibodies that recognize the extracellular epitope of the target protein. In a typical scenario, the extracellular domain of the transmembrane protein is first labeled with the primary antibody which is subsequently tagged with a QD conjugated to either a full secondary antibody or its antigen-binding fragment (Fab) (Figure 1A).The primary antibody bound to the target protein may also be labeled first with biotinylated secondary Fab fragments and then streptavidin-conjugated QDs. In another scenario, the primary antibody or its Fab fragment may be biotinylated and then used in conjunction with streptavidin-conjugated QDs. (Figure 1B) If a primary antibody against the target protein extracellular domain is not readily available, a hybrid strategy may be utilized, wherein the target protein is genetically modified to contain an extracellular peptide insert at the termini or within one of the extracellular loops (Hemagglutinin, AP peptide, SNAP-tag, Halotag) which is subsequently recognized by the complementary probe conjugated to QDs [2,3,22] (Figure 1D). In a method reported by our group in 2002, QDs are targeted to the cell surface neurotransmitter transporters through the use of high-affinity, selective small-molecule ligands [23] (Figure 1C). Our current ligand-conjugated QD strategy utilizes a transporter-specific organic ligand composed of (i) a high-affinity parent drug (agonist or antagonist) that enables targeting of specific binding sites within the transporter structure and facilitates pseudo-irreversible binding, (ii) a short alkyl spacer which provides sufficient flexibility and a suitable hydrophobic interface for a successful drug-binding site interaction, (iii) a PEG polymer that aids in aqueous solubility and prevents nonspecific binding to the plasma membrane, and (iv) a biotin terminus that is captured by streptavidin-conjugated QDs upon the successful transporter-ligand binding event [24–27]. To date, our lab has successfully demonstrated specific labeling of serotonin transporter (SERT), dopamine transporter (DAT), $GABA_c$ receptor, and D2 dopamine receptor (unpublished data) in either heterologous or endogenous expression systems [24–28].

When evaluating QD target specificity, we recommend a transfected monolayer culture as the starting system because the accessibility of target proteins is significantly reduced in a complex three-dimensional tissue (e.g., brain slice). Also, the ability to properly wash out the unbound QDs is severely impacted in the intact tissue samples. The target specificity of QD-antibody conjugates can be directly evaluated by preincubating the primary antibody

with the blocking peptide identical to the corresponding antigen sequence. In the case of ligand-conjugated QDs, the ligand-target interaction can be blocked by preincubating cells with a highaffinity antagonist (e. g., paroxetine for SERT). The use of non-transfected cells or small interfering RNA (siRNA) to silence the endogenous expression of the target molecule constitutes another important control, which allows one to determine the extent of nonspecific membrane binding. If the dynamic response of the target to an agonist or an antagonist is known, it is possible to indirectly test QD target specificity by modulating the behavior of the targeted molecule [29,30,11]. For instance, Varela et al. indirectly confirmed specific QD labeling of D1 dopamine receptors in cultured brain slices by observing the expected increase in D1 dopamine receptor diffusion rate after agonist administration [11]. One can also indirectly evaluate specific QD targeting by immobilizing target biomolecules via antibody crosslinking [31, 32]. When assessing QD target specificity in a complex sample, such as organotypic or acute brain slices, it might be necessary to implement a more quantitative approach. Biermann et al. introduced the “enrichment factor’ parameter, which is determined as the ratio of the number of QDs on transfected neurons in an organotypic brain slice to the number of QDs in the background [10].

2.2. Optical Implementation of a QD SPT Experiment.

Because a single QD is a robust and bright single photon emitter, optical implementation of a QD SPT experiment is fairly straightforward. Widefield optical microscopy has been the major workhorse in QD SPT due to its relative simplicity, lower cost, and readily attainable high frame rates (> 10 Hz). If QD diffusion occurs predominantly at the plasma membrane-coverslip interface, total internal reflection (TIR) mode can be used to generate a standing wave or “evanescent field” at the excitation point and thereby increase QD signal-to-noise ratio by eliminating out-of-focus intracellular autofluorescence. Another strategy to reduce background fluorescence is to utilize light-sheet illumination orthogonal to the objective and parallel to the imaging focal plane [33]. A high magnification (60x, or more) oil-immersion objective with a numerical aperture of ≥ 1.4 is typically used to yield images with the best signal-to-noise ratio (SNR) at the effective pixel size of ~100 nm. The new generation of back-illuminated complementary metal-oxide-semiconductor (CMOS) and electron-multiplying charge-coupled device (EMCCD) cameras with >90% quantum efficiency in the visible wavelength region and fast readout rates enable time-lapse single QD detection at integration times as low as several hundred microseconds with good SNR; however, a standard CCD, EMCCD, or CMOS camera is sufficient to achieve a benchmark frame rate of 30 Hz, allowing observation of such transient molecular events as receptor association with the membrane microdomains, stimulation-induced temporary arrest of receptor lateral diffusion (STALL), and receptor homo- or heterodimerization [3,7]. Broad absorption spectra and enormous extinction coefficients of QDs mean that a single QD can be excited with virtually any source, including mercury or xenon arc lamps, light-emitting diodes, and lasers. Although QD signal improves at lower wavelengths (350–400 nm) due to the increasing extinction coefficient, a commonly used 488 nm excitation wavelength offers an effective compromise between QD signal quality and excitation-induced cellular cytotoxicity. It is also important to keep the excitation intensity at a minimum to reduce QD blinking and cellular photodamage; generally, an intensity of ≤ 0.5 kW/cm^2 is appropriate. Finally, QDs emitting in the red region of the visible spectrum (600–700 nm), where cell

autofluorescence is low, are an optimal choice, as they readily facilitate parallel detection of GFP- or Alexa488-tagged biomolecules using the same excitation source in a multiplexed experiment [refer to ref. 34 and ref. 35 for excellent detailed guides on SPT instrumentation]. Next, we will illustrate the utility of QD SPT by discussing our recent key findings from the interrogation of the dynamic behavior of plasma membrane monoamine neurotransmitter transporters, a class of neuronal proteins critical to synaptic transmission, plasticity, behavior, and disease.

2.3. Preparation of Ligands for Conjugation to QDs.

The initial step of the ligand preparation is to select a suitable drug candidate. The drug molecule should possess high affinity for the protein target, with an optimal dissociation constant (K_D) below 10^{-8} M, high selectivity of binding to the target over structurally related proteins, and a convenient reactive handle for further synthetic modification. Previously, we identified a high-affinity, homotryptamine-based SERT antagonist, 3-(1,2,3,6-tetrahydropyridin-4-yl)-1H-indole, characterized by half-maximal inhibition (IC_{50}) of SERT-mediated serotonin uptake of 80 nM and featuring a basic nitrogen in the tetrahydropyridine ring amenable to conjugation. The synthetic route for generating biotinylated, PEGylated derivatives of 3-(1,2,3,6-tetrahydropyridin-4-yl)-1H-indole in Scheme 1 (Structures 1–9) [36]. Briefly, an alkyl chain spacer arm with 11 methylene units was attached to the basic nitrogen of the tetrahydropyridine ring by refluxing the parent drug with a phthalimide-protected alkyl bromide in acetonitrile in the presence of triethylamine. The phthalimide-protecting group was removed from the resulting products by treatment with hydrazine hydrate in ethanol to obtain the desired primary amine terminus. The intermediate was then coupled to biotin-PEG5000-Succinimidyl NHS ester to get the final crude product (IDT357). The crude product was purified by preparative HPLC and characterized by MALDI mass spectrometry. The biological activity of the biotinylated IDT357 was assessed using a two-step QD labeling protocol (Figure 2A). The stably transfected SERT-expressing HEK293T cells grown in MatTek dishes were first labeled with 500 nM of the desired SERT ligand in the labeling buffer for 10 minutes, washed several times with ligand-free labeling buffer, and then incubated with a 1 nM solution of Qdot655 streptavidin conjugate in a 1% BSA (bovine serum albumin) imaging buffer for 5 minutes. The cells were then washed 3–5 times with QD-free imaging buffer to remove any unbound QDs and imaged immediately on a Zeiss widefiled epifluorescence microscope. A representative fluorescence image of hSERT-expressing cells labeled with biotinylated IDT357 and QD-streptavidin conjugates is shown in Figure 2B. Successful labeling was apparent from a characteristic membrane-associated fluorescence, whereas the SERT-expressing cells preblocked with paroxetine, a high-affinity SERT inhibitor, displayed no such fluorescence. In addition to lower-magnification, whole-cell measurements, we also confirmed specific IDT357-mediated QD targeting of SERT by imaging YFP-SERT-transfected HEK293 cells using lower QD density and a 60x objective in the absence and presence of 10 μM paroxetine (Figure 2C). Paroxetine preblock eliminated virtually all of QD binding to SERT expressing cells, enabling the investigation of SERT diffusion dynamics reported in section 3.3.

3.1. QD-tagged Serotonin Transporters are Associated with Membrane Microdomains.

The presynaptic, antidepressant-sensitive SERT has emerged as a major determinant of an individual's risk of neuropsychiatric illness [37]. Although biochemical studies have shown that regulation of SERT activity is intimately linked to its residence in specialized, cholesterol- and GM1 ganglioside-rich membrane microdomains, investigation of the spatiotemporal membrane organization of single SERT proteins has been hampered by the poor resolution of available methods [25]. To this end in 2012, our group reported the first use of the ligand-conjugated QD labeling strategy to capture the plasma membrane dynamics of single SERT proteins endogenously expressed in immortalized serotonergic rat neurons RN46A [25]. The first measurement of single SERT diffusion provided direct proof that SERT exists as two distinct pools in the membrane of untreated RN46A cells, with the dominant fraction (~90%) displaying highly restricted diffusion and the remaining pool diffusing at a significantly faster rate in an unconstrained manner. Parallel imaging of Alexa488-tagged cholera toxin B, a marker of cholesterol- and GM1 ganglioside-rich membrane microdomains, demonstrated a high degree of SERT-QD colocalization with cholera toxin B membrane patches. Partial cholesterol depletion of RN46A cells with methyl-β-cyclodextrin, a cyclic glucose oligomer capable of sequestering membrane cholesterol, resulted in a dramatic increase in the overall diffusion rate and a complete loss of the restricted SERT pool, indicating that the restricted diffusion of SERT under basal conditions stems from its localization to the membrane microdomains (Figure 3). Lateral acceleration of SERT proteins after cholesterol depletion was accompanied by a pronounced dispersal of cholera toxin B membrane patches. By applying the 5-second radial displacement analysis to single SERT trajectories, we determined that the overwhelming majority of SERT proteins under basal conditions reside in the putative microdomains approximately 500 nm in diameter. Furthermore, the restricted SERT pool appeared to be under the constitutive control of p38 mitogen-activated protein kinase (p38 MAPK) pathway. The mammalian p38 MAPK family is a group of intracellular kinase enzymes mediating cellular response to various stressors (UV radiation, inflammatory cytokines, heat shock, osmotic shock) and promoting an increase in SERT transport activity in part through phosphorylation, a biochemical event that involves the addition of a phosphate group to the serine, threonine and tyrosine side chains [38]. We observed that activation of the p38 MAPK pathway induced accelerated SERT lateral movement, with the majority of SERT proteins remaining constrained in the putative membrane microdomains. The effects of actin cytoskeleton disruption on SERT mobility were analogous to those observed during p38 MAPK activation, prompting us to hypothesize that catalytic SERT activation proceeds via partial dissociation of SERT proteins from the actin cytoskeleton within the cholesterol- and GM1 ganglioside-rich membrane microdomains. Our findings demonstrated that QD SPT is capable of illuminating the molecular details of pharmacological manipulation and catalytic activation of single proteins in living cells occurring over milliseconds to seconds at the nanoscale.

3.2. QDs Reveal Altered Diffusion Dynamics of the ADHD-Associated Arg615Cys Dopamine Transporter Coding Variant.

In another application of the ligand-conjugated QD labeling approach, we established the dynamic imaging of membrane dopamine transporter (DAT) proteins at the single-molecule

level for the first time [27]. DAT is the primary mechanism of shaping synaptic dopaminergic transmission, as it actively clears extracellular dopamine into the presynaptic terminals [39]. Notably, DAT is the primary target for drugs of abuse such as cocaine and amphetamine as well as therapeutic drugs such as methylphenidate (Ritalin) [39–43]. Naturally occurring DAT coding variation reported in subjects diagnosed with the attention deficit/hyperactivity disorder (ADHD), autism spectrum disorder (ASD), and infantile Parkinsonism causes anomalous dopamine efflux, complete loss of function, or trafficking dysregulation [40–43]. We sought to apply the ligand-conjugated QD SPT framework to investigate the membrane dynamics of the ADHD-derived R615C DAT variant. This DAT mutant features an argninine-to-cysteine substitution at position 615 in the intracellular C-terminus and had been previously shown in ensemble experiments to redistribute away from the GM1 ganglioside-rich membrane microdomains [40]. QD SPT analysis of the diffusion dynamics of the wildtype and R615C DAT proteins in a stably transfected HEK293 cell line revealed that the ADHD-derived DAT variant exhibited accelerated membrane movement in contrast to the wildtype DAT protein (Figure 4). The accelerated basal membrane dynamics were accompanied by the failure of the R615C DAT proteins to mobilize after lipid raft disruption achieved through partial cholesterol depletion, whereas the diffusion rate of the wildtype DAT after partial cholesterol depletion was comparable to that of the R615C variant under basal conditions. Additionally, the administration of amphetamine, a potent multifaceted DAT modulator, failed to mobilize the R615C DAT proteins as opposed to the wildtype DAT, consistent with the previously observed insensitivity of the R615C variant to amphetamine-induced internalization. Together, these QD SPT findings point to a membrane microdomain mislocalization of the ADHD-associated DAT mutant that is likely driven by the transporter's constitutively hyperphosphorylated status.

3.3. QDs Reveal Altered Diffusion Dynamics of the Autism-Associated Gly56Ala SERT Coding Variant.

Multiple naturally-occurring, brain disorder-associated coding variants have also been identified for the SERT protein, fundamentally altering transporter function and regulation [44]. One such gain-of-function variant, Gly56Ala (G56A) SERT, has been associated with autism spectrum disorder (ASD), a highly prevalent brain disorder characterized by impaired social communication and abnormal sensory processing [44,45]. In fact, the G56A allele is carried by approximately 1 in 200 Caucasian subjects, representing more than a million Americans. G56A SERT displays an elevated constitutive phosphorylation rate and the complete loss of sensitivity to p38 MAPK-mediated phosphorylation, thus enabling the investigation of the direct link between the transporter phosphorylation status and its lateral mobility [45].

To capture membrane dynamics of G56A and WT SERT in stably transfected Chinese hamster ovary (CHO) cells, a biotinylated, SERT-selective ligand IDT357 was used in conjunction with streptavidin-conjugated QDs as described in Section 2.2 and SI. Membrane movement of QD-tagged SERTs was recorded for 1 minute at the acquisition rate of 10 Hz, and the motion parameters were then extracted from the obtained trajectories. The hyperphosphorylated G56A SERT mutant showed significantly higher rate of diffusion compared to the wild type SERT ($0.016 \pm 0.001\ \mu m^2/s$ versus $0.011 \pm 0.001\ \mu m^2/s$, $p<0.001$,

Kolmogorov-Smirnov statistical test) (Fig. 5 A and B). To visualize the extent of lateral movement of QD-tagged SERT proteins from the starting position over a 5s recording interval (5-sec dr), we plotted radial displacement of each variant in Figure 5. The G56A variant traveled slightly but significantly farther than wild type SERT (one-way ANOVA, $p<0.01$) (Fig. 5 C and D). We hypothesize that the mutation to alanine disrupts G56A SERT membrane microdomain localization and key associations with the SERT membrane interactome, resulting in a dysregulated dynamic phenotype. Interestingly, in addition to the abnormal diffusion dynamics exhibited by brain disorder-associated DAT and SERT variants in our studies, Jezequel *et al.* recently determined that circulating autoantibodies derived from the blood serum of psychotic patients diagnosed with schizophrenia directly destabilize surface dynamics and nanoscale organization of the synaptic glutamate NMDA receptors [46]. We believe that spatiotemporal membrane disorganization of neuronal proteins is emerging as a central molecular pathological theme in brain disorder research (Table 2).

3.4. QD-Based Approach to Survey 3D Distribution and Dynamics of Endocytosed Transporters.

Decades of research efforts aimed at unraveling the intricacies of neurotransmitter transporter trafficking support the notion that membrane pool of transporters is in constant flux, and proper transporter turnover represents an important modulatory mechanism of synaptic plasticity. Membrane transporters undergo marked constitutive and regulated redistribution away from the plasma membrane driven in part by amino-/carboxy-terminal linear motifs, conformational shifts, and covalent modifications [47–49]. Although transporter turnover is an essential component of neurotransmission, the intracellular dynamics and subsequent fate of individual transporters remain poorly understood. Our ligand-conjugated QD approach is uniquely suited to interrogate the intracellular dynamics of transporters in living cells because (i) pseudoirreversible ligand binding ensures that the transporter-QD complex remains intact post-endocytosis and (ii) bright and stable QD signal enables prolonged observation of single cargo trafficking [26,27]. A proof-of-concept implementation of our QD labeling approach together with spinning-disk confocal microscopy to investigate DAT endocytic trafficking is shown in Figure 6A. Notably, the spinning-disk microscope is equipped with a z-axis piezo nanopositioning stage, which enabled capture of transient endocytic events and robust single cargo localization analysis. At z-speeds of 10 300-nm steps per second, 3D image stacks were acquired to detect QD-DAT complexes relative to the plasma membrane of transiently transfected HEK293 cells, conveniently labeled with a CellMask™ lipophilic membrane stain (Fig 6B) (refer to SI for experimental details). Binarizing the acquired z-stacks and performing 2-channel colocalization analysis allows us to discriminate intracellular QDs from those localized to the plasma membrane (Fig 6C-E). By incorporating an additional fluorescent marker of early recycling endosomes or late degradative compartments, our approach could be a valuable tool for quantitative determination of DAT intracellular fate at the single-cargo level in 3D. Furthermore, time-lapse imaging of a single-plane cross-section of a cell with internalized QD-DAT complexes permits quantitation of single cargo movement at millisecond temporal resolution with exceptional SNR (Figure 7).

4. Challenges and Prospects.

4.1. Size.

Commercially available biofunctionalized QDs are comprised of an inorganic core/shell, an amphiphilic polymer shell, a PEG layer, and multiple copies of either a divalent antibody or a tetravalent streptavidin on the surface. Together, these components contribute to the complex QD architecture far exceeding the hydrodynamic diameter of 20 nm and the molecular mass of 1,000,000 Da [2]. In fact, these dimensions are several orders of magnitude larger than the size of a typical membrane protein target (5–10 nm and 50–100 kDa). Therefore, it is a valid concern that a bulky and polyvalent QD probe might restrict access to the crowded cellular compartments (e.g., synaptic cleft) and influence the intrinsic diffusion pattern of the targeted biomolecule. To date, several groups have systematically examined this issue, and the results have been conflicting. Domanov et al. demonstrated that the viscous drag on a QD bound to a protein is dominated by the mobility of the target anchored in the membrane [64]. Pierobon et al. explored the QD drag effects when tagged to a molecular motor myosin V and determined that the size of the probe does not affect the motion and processivity of myosin V [65]. Groc et al. found that the diffusion rate of extrasynaptic glutamate receptors tagged with QD-antibody conjugates did not differ significantly from that of receptors tagged with either dye-conjugated antibodies or small peptides [66]. However, Groc et al. also reported that the fraction of synaptic QD-tagged glutamate receptors was significantly reduced compared to dye-tagged receptors [66]. This finding was recently corroborated by Lee et al. that observed nearly complete elimination of the mobile pool of extrasynaptic glutamate receptors when replacing commercial QDs with custom-made compact QDs or Atto dyes [67]. Nechyporuk-Zloy et al. reported that QDs slowed down the membrane diffusion and changed the type of motion of potassium channels when compared directly to Alexa488 dye [68]. In addition, Howarth et al. discovered that commercial streptavidin-conjugated QDs limited the access of glutamate receptors to the synaptic cleft and triggered surface clustering and internalization of the surface ephrin receptor [69]. Recently, Abraham et al. demonstrated that Fab-conjugated QDs hinder B cell receptor diffusion on multiple glass coating substrates when compared directly to Cy3-Fab conjugates [70]. It appears that the large QD size might significantly perturb the intrinsic diffusivity of the targeted biomolecule, and it is therefore imperative that one performs an orthogonal tracking experiment to validate the diffusion dynamics observed via QD SPT. In parallel, synthetic efforts have been under way to reduce QD size; the primary focus is on replacing the bulky amphiphilic polymer shell with low molecular weight polymers [71] or displacing the native hydrophobic ligands with mono- and bidentate PEGylated alkanethiols [67,72]. Another alternative is the use of imidazole-based block copolymers [73]. Recently, Farlow et al. utilized the affinity of phosphorothioate oligonucleotides for the semiconductor surface to prepare monovalent DNA-functionalized QDs [74]. However, the generation of compact QDs typically requires stripping of native organic ligands which renders compact QDs prone to aggregation and negatively affects optical properties [71,73]. Also, smaller size as a rule results in increased nonspecific binding. As such, the research efforts to date have yet to result in a commercially viable class of compact QDs.

4.2. Blinking.

Even under constant illumination, almost all colloidal nanocrystals exhibit a signature stochastic intermittency in their photoluminescence spectra, a phenomenon first observed by Nirmal et al. [75] Currently, it is widely accepted that QD blinking appears to originate from the illumination-induced trapping of a charge carrier either within or at the surface of the QD ("on" → "off"), and subsequent nonradiative recombination neutralizes the charged QD and returns it to the emissive state ("off" → "on") [76]. In the context of SPT experiments, QD blinking serves as a useful criterion to ensure the observation of single nanocrystal species. On the other hand, QD blinking does not allow the recording of trajectories as a continuum; this disadvantage necessitates the use of advanced algorithms to minimize false correspondence of trajectory segments. Systematic study of the "on"/"off" emissive state switching revealed a pronounced dependency on the excitation intensity, excitation wavelength, shell composition, and shell thickness [76–78]. Our group developed a correlation technique that utilizes widefield optical microscopy and atomic number contrast scanning transmission electron microscopy (Z-STEM) to directly interrogate the contribution of the internal and surface QD defects to the rate of nonradiative recombination [77,78]. Synthetic control of QD blinking rate has been pursued by multiple groups; blinking suppression can be achieved by passivating QD cores with a thick multilayer shell and/or interfacial alloying that results in a smooth radial QD composition change and consequently in a soft confinement potential [77]. These new blinking-suppressed materials represent an attractive option for SPT experiments, as they would eliminate the need to account for gaps during trajectory reconstruction. In some cases, the stochastic nature of blinking is desirable and facilitates super-resolution imaging of diffraction-limited QD spots separated by nanometer distances [79]. Furthermore, we anticipate that achieving precise synthetic control over the QD blinking rate will potentially enable single-channel, super-resolution multiplexing of biomolecules tagged with fast-blinking and slow-blinking QDs using standard instrumentation.

4.3. Competing Technologies.

We would be remiss not to acknowledge recent advances in the realm of organic dye- and fluorescent protein-based super-resolution imaging. In fact, the predominance of QDs in the SPT studies in the monolayer culture has been considerably diminished with the advent of brighter, more photostable dyes [80] and the proliferation of the alternative tracking methods based on the stochastic single-molecule localizations [7]. Although QD photostability underlies the ability to monitor prolonged QD diffusion, it is now possible to obtain high-resolution tracks of dye-tagged biomolecules at millisecond time resolution, even for as long as 7 minutes in reduced oxygen environment [81]. Nevertheless, we are confident that QDs will remain the probe of first choice in multiplexing experiments and in applications that require very bright and photostable probes, such as 3D SPT or tracking in *ex vivo* tissue slices or *in vivo*.

Conclusions.

Since its advent in 1980s, SPT provided a powerful experimental avenue to directly examine important biological events in living cells at the length and time scales elusive to the

ensemble biochemical techniques. QD technology has been an integral element of the groundbreaking success of SPT, owing to the superior photophysical performance of single QD emitters. Since the seminal report of Dahan *et al.* in 2003, QD SPT revolutionized our understanding of the dynamic plasma membrane architecture, shed light on the composition and assembly of synaptic supramolecular protein complexes, unraveled the molecular mechanisms of viral entry into living cells, and mapped out the initial signaling events involved in the innate immune response. In the same period of time, our lab developed the ligand-conjugated QD labeling strategy to target transmembrane neurotransmitter transporters and applied the QD SPT framework to decipher the dynamic membrane organization of the transporters. Importantly, our QD SPT studies have identified a direct functional impact of the brain disorder-associated coding variation on transporter membrane diffusion dynamics, supporting pathogenic relevance of dysregulated surface trafficking of proteins involved in neurotransmission. We envision that the enormous QD photon budget will permit examining molecular interactions at the micro- to – millisecond timescale in native 3D environment *ex vivo* and ultimately *in vivo*.

Acknowledgement.

This work was supported by NIH Grant EB003728 to SJR. The authors would like to thank Dr. James McBride for critical manuscript edits, Dr. Randy Blakely for providing stably transfected SERT-WT and SERT-G56A CHO cells, Dr. Jerry Chang for useful discussions regarding SPT experiments and imaging, Dr. Jay Forsythe and Dr. John McLean for assistance with MALDI mass spectrometry, and Dr. Ruth McNees and Dr. Brian Bachmann for help with HPLC purification. DMB was supported by the NSF Graduate Research Fellowship Program DGE-1445197, LBT was supported by the CBI Training Grant (NIH T32GM065086–14), and LH was supported by the Vanderbilt Institute of Chemical Biology Summer REU program. Fluorescence microscopy experiments were performed in part through the use of the VU Cell Imaging Shared Resource (supported by NIH grants CA68485, DK20593, DK58404, DK59637 and EY08126). Flow Cytometry experiments were performed through the use of the VMC Flow Cytometry Shared Resource supported by the Vanderbilt Ingram Cancer Center (P30 CA68485) and the Vanderbilt Digestive Disease Research Center (DK058404).

*Author Biographies

Dr. Sandy Rosenthal’s Biography:

Dr. Sandra Rosenthal received a BS with Honors in Chemistry while playing four years of Division 1 basketball for Valparaiso University. She earned her PhD from the University of Chicago in 1993 and accepted a NSF Postdoctoral Fellowship in Chemistry that she took to UC Berkeley and Lawrence Berkeley National Laboratory. In 1996 Dr. Rosenthal joined the chemistry faculty of Vanderbilt University as an assistant professor and is now the Jack and Pamela Egan Professor of Chemistry, Professor of Physics and Astronomy, Pharmacology, Chemical and Biomolecular Engineering, Materials Science, and the Director of the Vanderbilt Institute of Nanoscale Science and Engineering (VINSE). She has recently been awarded the Herty Medal of the Georgia Section of the American Chemical Society and the Southeastern Conference (SEC) Faculty Achievement Award. One of Professor Rosenthal’s passions is to realize precision medicine for mental illnesses. To this end, a major focus of her research is to develop and use nanotechnology to elucidate molecular mechanisms of mental illness.

Dr. Oleg Kovtun's Biography:

Dr. Oleg Kovtun received his B. S. in Chemistry summa cum laude from Murray State University in 2007, followed by a Ph.D. in Chemistry from Vanderbilt University in 2013, where he pursued studies of the dopamine transporter membrane dynamics using antagonist-conjugated quantum dots under the direction of Dr. Sandy Rosenthal and Dr. Randy Blakely. Following his graduate studies, Dr. Kovtun worked as an analytical GC/GC-MS/HPLC chemist at McCoy & McCoy Laboratories, where he was responsible for determining the levels of trace organic contaminants in samples collected for regulatory compliance reporting and industry QC. Dr. Kovtun returned to the Rosenthal lab in 2015 to pursue postdoctoral training. The central aim of his current research is to illuminate the molecular factors underlying neurotransmitter transporter and receptor dynamic dysregulation in mental illness through the use of quantum dots.

References.

1. Genger-Resch U, Grabolle M, Cavaliere-Jaricot S, Nitschke R, Nann T, Quantum dots versus organic dyes as fluorescent labels, Nat. Methods 5 (2008) 763–775. [PubMed: 18756197]
2. Rosenthal SJ, Chang JC, Kovtun O, McBride JR, Tomlinson ID, Biocompatible quantum dots for biological applications, Chem. Biol 18 (2011) 10–24. [PubMed: 21276935]
3. Pinaud F, Clarke S, Sittner A, Dahan M, Probing cellular events, one quantum dot at a time, Nat. Methods 7 (2010) 275–285. [PubMed: 20354518]
4. Bruchez M, Jr., Moronne M, Gin P, Weiss S, Alivisatos AP, Semiconductor nanocrystals as fluorescent biological labels, Science 281 (1998) 2013–2016. [PubMed: 9748157]
5. Chan WC, Nie S, Quantum dot bioconjugates for ultrasensitive nonisotopic detection, Science 281 (1998) 2016–2018. [PubMed: 9748158]
6. Dahan M, Levi S, Luccardini C, Rostaing P, Riveau B, Triller A, Diffusion dynamics of glycine receptors revealed by single-quantum dot tracking, Science 302 (2003) 442–445. [PubMed: 14564008]
7. Kusumi A, Tsunoyama TA, Hirosawa KM, Kasai RS, Fujiwara TK, Tracking single molecules at work in living cells, Nat. Chem. Biol 10 (2014) 524–532. [PubMed: 24937070]
8. Choquet D, Triller A, The dynamic synapse, Neuron 80 (2013) 691–703. [PubMed: 24183020]

9. Cutler PJ, Malik MD, Liu S, Byars JM, Lidke DS, Lidke KA, Multi-color quantum dot tracking using a high-speed hyperspectral line-scanning microscope, PLoS One 8 (2013) e64320. [PubMed: 23717596]
10. Biermann B, Sokoll S, Klueva J, Missler M, Wiegert JS, Sibarita JB, Heine M, Imaging of molecular surface dynamics in brain slices using single-particle tracking, Nat. Commun 5 (2014) 3024. [PubMed: 24429796]
11. Varela JA, Dupuis JP, Etchepare L, Espana A, Cognet L, Groc L, Targeting neurotransmitter receptors with nanoparticles in vivo allows single-molecule tracking in acute brain slices, Nat. Commun 7 (2016) 10947. [PubMed: 26971573]
12. Holtzer L, Meckel T, Schmidt T, Nanometric three-dimensional tracking of individual quantum dots in cells, Appl. Phys. Lett 90 (2007) 053902–1–053902–3.
13. Thompson MA, Lew MD, Badieirostami M, Moerner WE, Localizing and tracking single nanoscale emitters in three dimensions with high spatiotemporal resolution using a double-helix point spread function, Nano Lett 10 (2010) 211–218. [PubMed: 20000821]
14. Ram S, Prabhat P, Chao J, Ward ES, Ober RJ, High accuracy 3D quantum dot tracking with multifocal plane microscopy for the study of fast intracellular dynamics in live cells, Biophys. J 95 (2008) 6025–6043. [PubMed: 18835896]
15. Clausen MP, Lagerholm BC, Visualization of plasma membrane compartmentalization by high-speed quantum dot tracking, Nano Lett 13 (2013) 2332–2337. [PubMed: 23647479]
16. Saxton MJ, A biological interpretation of transient anomalous subdiffusion. I. Qualitative model, Biophys. J 92 (2007) 1178–1191. [PubMed: 17142285]
17. Saxton MJ, A biological interpretation of transient anomalous subdiffusion. II. Reaction kinetics, Biophys. J 94 (2008) 760–771. [PubMed: 17905849]
18. Weigel AV, Simon B, Tamkun MM, Krapf D, Ergodic and nonergodic processes coexist in the plasma membrane as observed by single-molecule tracking, Proc. Natl. Acad. Sci. USA 108 (2011) 6438–6443. [PubMed: 21464280]
19. Zanetti-Domingues LC, Tynan CJ, Rolfe DJ, Clarke DT, Martin-Fernandez M, Hydrophobic fluorescent probes introduce artifacts into single-molecule tracking experiments due to non-specific binding, PLoS One 8 (2013) e74200. [PubMed: 24066121]
20. Chang JC, Rosenthal SJ, Visualization of lipid raft membrane compartmentalization in living RN46A neuronal cells using single quantum dot tracking, ACS Chem. Neurosci 3 (2012) 737–743. [PubMed: 23077717]
21. Bentzen EL, Tomlinson ID, Mason J, Gresch P, Warnement MR, Wright D, Sanders-Bush E, Blakely RD, Rosenthal SJ, Surface modification to reduce nonspecific binding of quantum dots in live cell assays, Bioconjug. Chem 16 (2005) 1488–1494. [PubMed: 16287246]
22. Chang JC, Kovtun O, Blakely RD, Rosenthal SJ, Labeling of neuronal receptors and transporters with quantum dots, Wiley Interdiscip. Rev. Nanomed. Nanobiotechnol 4 (2012) 605–619. [PubMed: 22887823]
23. Rosenthal SJ, Tomlinson I, Adkins EM, Schroeter S, Adams S, Swafford L, McBride J, Wang Y, DeFelice LJ, Blakely RD, Targeting cell surface receptors with ligand-conjugated nanocrystals, 124 (2002) 4586–4594.
24. Chang JC, Tomlinson ID, Warnement MR, Iwamoto H, DeFelice LJ, Blakely RD, Rosenthal SJ, A fluorescence displacement assay for antidepressant drug discovery based on ligandconjugated quantum dots, 133 (2011) 17528–17531.
25. Chang JC, Tomlinson ID, Warnement MR, Ustione A, Carneiro AM, Piston DW, Blakely RD, Rosenthal SJ, Single molecule analysis of serotonin transporter regulation using antagonist-conjugated quantum dots reveals restricted, p38 MAPK-dependent mobilization underlying uptake activation, J. Neurosci 32 (2012) 8919–8929. [PubMed: 22745492]
26. Kovtun O, Tomlinson ID, Sakrikar DS, Chang JC, Blakely RD, Rosenthal SJ, Visualization of the cocaine-sensitive dopamine transporter with ligand-conjugated quantum dots, ACS Chem. Neurosci 2 (2011) 370–378. [PubMed: 22816024]
27. Kovtun O, Tomlinson ID, Sakrikar D, Chang JC, Arzeta-Ferrer X, Blakely RD, Rosenthal SJ, Single-quantum-dot tracking reveals altered membrane dynamics of an attention-deficit/

hyperactivity disorder-derived dopamine transporter coding variant, ACS Chem. Neurosci 6 (2015) 526–534. [PubMed: 25747272]

28. Gussin HA, Tomlinson ID, Little DM, Warnement MR, Qian H, Rosenthal SJ, Pepperberg DR, Binding of muscimol-conjugated quantum dots to GABAC receptors, J. Am. Chem. Soci 128 (2006) 15701–15713.
29. Bannai H, Levi S, Schweizer C, Inoue T, Launey T, Racine V, Sibarita JB, Mikoshiba K, Triller A, Neuron 62 (2009) 670–682. [PubMed: 19524526]
30. Murphy-Royal C, Dupuis JP, Varela JA, Panatier A, Pinson B, Baufreton J, Groc L, Oliet SH, Surface diffusion of astrocytic glutamate transporters shapes synaptic transmission, J. Neurosci 18 (2015) 219–226.
31. Heine M, Groc L, Frischknecht R, Beique JC, Lounis B, Rumbaugh G, Huganir RL, Cognet L, Choquet D, Surface mobility of postsynaptic AMPARs tunes synaptic transmission, Science 320 (2008) 201205.
32. Dupuis JP, Ladepeche L, Seth H, Bard L, Varela J, Mikasova L, Bouchet D, Rogemond V, Honnorat J, Hanse E, Groc L, Surface dynamics of GluN2B-NMDA receptors controls plasticity of maturing glutamate synapses, EMBO J 33 (2014) 842–861. [PubMed: 24591565]
33. Friedrich M, Nozadze R, Gan Q, Zelman-Femiak M, Ermolayev V, Wagner TU, Harms GS, Detection of single quantum dots in model organisms with sheet illumination microscopy, Biochem. Biophys. Res. Commun 390 (2009) 722–727. [PubMed: 19833091]
34. Walter NG, Huang CY, Manzo AJ, Sobhy MA, Do-it-yourself guide: how to use the modern singlemolecule toolkit, Nat. Methods 5 (2008) 475–489. [PubMed: 18511916]
35. Deschout H, Cella Zanacchi F, Mlodzianoski M, Diaspro A,.Bewersdorf J, Hess ST, Braeckmans K, Precisely and accurately localizing single emitters in fluorescence microscopy, Nat. Methods 11 (2014) 253–266. [PubMed: 24577276]
36. Tomlinson ID, Mason JN, Blakely RD, Rosenthal SJ, Inhibitors of the serotonin transporter protein (SERT): the design and synthesis of biotinylated derivatives of 3-(1,2,3,6-tetrahydro-pyridin-4-yl)-1H indoles. High-affinity serotonergic ligands for conjugation with quantum dots, Bioorg. Med. Chem. Lett 15 (2005) 5307–5310. [PubMed: 16183285]
37. Murphy DL, Fox MA, Timpano KR, Moya PR, Ren-Patterson R, Andrews AM, Holmes A, Lesch KP, Wendland JR, How the serotonin story is being rewritten by new gene-based discoveries principally related to SLC6A4, the serotonin transporter gene, which functions to influence all cellular serotonin systems, Neuropharmacology 55 (2008) 932–960. [PubMed: 18824000]
38. Zhu CB, Carneiro AM, Dostmann WR, Hewlett WA, Blakely RD, p38 MAPK activation elevates serotonin transport activity via a trafficking—independent, protein phosphatase 2A-dependent, J. Biol. Chem 280 (2005) 15649–15658. [PubMed: 15728187]
39. Schmitt KC, Reith MEA, Regulation of the dopamine transporter, Ann. N. Y. Acad. Sci 1187 (2010) 316– 340. [PubMed: 20201860]
40. Mazei-Robison MS, Bowton E, Holy M, Schmudermaier M, Fressmuth M M., Sitte HH, Galli A, Blakely RD, Anomalous dopamine release associated with a human dopamine transporter coding variant, J. Neurosci 28 (2008) 7040–7046. [PubMed: 18614672]
41. Bowton E, Saunders C, Erreger K, Sakrikar D, Matthhies HJ, Sen N, Jessen T, Colbran RJ, Caron MG, Javitch JA, Blakely RD, Galli A, Dysregulation of dopamine transporters via dopamine D2 autoreceptors triggers anomalous dopamine efflux associated with attention-deficit hyperactivity disorder, J. Neurosci 30 (2010) 6048–6057. [PubMed: 20427663]
42. Sakrikar D, Mazei-Robison MS, Mergy MA, Richtand NW, Han Q, Hamilton PJ, Bowton E, Galli A, Veenstra-Vanderweele J, Gill M, Blakely RD, Attention deficit/hyperactivity disorder-derived coding variation in the dopamine transporter disrupts microdomain targeting and trafficking regulation, J. Neurosci 32 (2012) 5385–5397. [PubMed: 22514303]
43. Hansen FH, Skjorringe T, Yasmeen S, Arends NV, Sahai MA, Erreger K, Andreassen TF, Holy M, Hamilton PJ, Neergheen V, Karlsborg M, Newman AH, Pope S, Heales SJ, Friberg L, Law I, Pinborg LH, Sitte HH, Loland C, Shi L, Weinstein H, Galli A, Hjermind LE, Moller LB, Gether U, Missense dopamine transporter mutations associate with adult parkinsonism and ADHD, J. Clin. Invest 124 (2014) 3107–3120. [PubMed: 24911152]

44. Prasad HC, Steiner JA, Sutcliffe JS, Blakely RD, Enhanced activity of human serotonin transporter variants associated with autism, Philos. Trans. R. Soc. Lond. B. Biol. Sci 364 (2009) 163–173. [PubMed: 18957375]
45. Prasad HC, Zhu CB, McCauley JL, Samuvel DJ, Ramamoorthy S, Shelton RC, Hewlett WA, Sutcliffe JS, Blakely RD, Human serotonin transporter variants display altered sensitivity to protein kinase G and p38 mitogen-activated protein kinase, Proc. Natl. Acad. Sci. USA 102 (2005) 11545–11550. [PubMed: 16055563]
46. Jezequel J, Johansson EM, Dupuis JP, Rogemond V, Grea H, Kellermayer B, Hamdani N, Le Guen E, Rabu C, Lepleux M, Spatola M, Mathias E, Bouchet D, Ramsey AJ, Yolken RH, Tamouza R, Dalmau J, Honnorat J, Leboyer M, Groc L, Dynamic disorganization of synaptic NMDA receptors triggered by autoantibodies from psychotic patients, Nat. Commun 8 (2017) 1791. [PubMed: 29176681]
47. Melikian HE, Neurotransmitter transporter trafficking: endocytosis, recycling, and regulation, Pharmacol. Ther 104 (2004) 17–27. [PubMed: 15500906]
48. Eriksen J, Bjorn-Yoshimoto WE, Jorgensen TN, Newman AH, Gether U, Postendocytic sorting of constitutively internalized dopamine transporter in cell lines and dopaminergic neuros, J. Biol. Chem 285 (2010) 27289–27301. [PubMed: 20551317]
49. Bermingham DP, Blakely RD, Kinase-dependent regulation of monoamine neurotransmitter transporters, Pharmacol. Rev 68 (2016) 888–953. [PubMed: 27591044]
50. Lacoste TD, Michalet X, Pinaud F, Chemla DS, Alivisatos AP, Weiss S, Ultrahigh-resolution multicolor colocalization of single fluorescent probes, PNAS 97 (2000) 9461–9466. [PubMed: 10931959]
51. Wu X, Liu H, Liu J, Haley KN, Treadway JA, Larson JP, Ge N, Peale F, Bruchez MP, Immunofluorescent labeling of cancer marker Her2 and other cellular targets with semiconductor quantum dots, Nature Biotechnology 21 (2003) 41–46.
52. Lidke DS, Lidke KA, Rieger B, Jovin TM, Arndt-Jovin DJ, Reaching out for signals: filopodia sense EGF and respond by directed retrograde transport of activated receptors, J. Cell. Biol 170 (2005) 619–626. [PubMed: 16103229]
53. Courty S, Luccardini C, Bellaiche Y, Cappello G, Dahan M, Tracking individual kinesin motors in living cells using single quantum-dot imaging, Nano Lett 6 (2006) 1491–1495. [PubMed: 16834436]
54. McBride JR, Treadway J, Feldman LC, Pennycook SJ, Rosenthal SJ, Structural basis for near unity quantum yield core/shell nanostructures, Nano Lett 6 (2006) 1496–1501. [PubMed: 16834437]
55. Zhang Q, Li Y, Tsien RW, The dynamic control of kiss-and-run and vesicular reuse probed with single nanoparticles, Science 322 (2009) 1448–1453.
56. Hoyer P, Staudt T, Engelhardt J, Hell SW, Quantum dot blueing and blinking enables fluorescence nanoscopy, Nano Lett 11 (2011) 245–250. [PubMed: 21128678]
57. Sokoll S, Prokazov Y, Hanses M, Biermann B, Tonnies K, Heine M, Fast three-dimensional singleparticle tracking in natural brain tissue, Biophys. J 109 (2015) 1463–1471. [PubMed: 26445447]
58. Hanne J, Falk HJ, Gorlitz F, Hoyer P, Engelhardt J, Sahl SJ, Hell SW, STED nanoscopy with fluorescent quantum dots, Nat. Commun 6 (2015) 7127. [PubMed: 25980788]
59. De Koninck P, Labrecque S, Heyes CD, Wiseman PW, Probing synaptic signaling with quantum dots, HFSP J 1 (2007) 5–10. [PubMed: 19404455]
60. Rust MB, Gurniak CB, Renner M, Vara H, Morando L, Gorlich A, Sassoe-Pognetto M, Banchaabouchi MA, Giustetto M, Triller A, Choquet D, Witke W, Learning AMPA receptor mobility and synaptic plasticity depend on n-cofilin-mediated actin dynamics, EMBO J 29 (2010) 1889–1902. [PubMed: 20407421]
61. Valentine CD, Lukacs GL, Verkman AS, Haggie PM, Reduced PDZ interactions of rescued ΔF508CFTR increases its cell surface mobility, J. Biol. Chem 287 (2012) 43630–43638. [PubMed: 23115232]
62. Pathania M, Davenport EC, Muir J, Sheehan DF, Lopez-Domenech G, Kittler JT, The autism and schizophrenia associated gene CYFIP1 is critical for the maintenance of dendritic complexity and the stabilization of mature spines, Transl. Psychiatry 4 (2014) e374. [PubMed: 24667445]

63. Zhang H, Zhang C, Vincent J, Zala D, Benstaali C, Sainlos M, Grillo-Bosch D, Daburon S, Coussen F, Cho Y, David DJ, Saudou F, Humeau Y, Choquet D, Pharmacological modulation of AMPA receptor surface diffusion restores hippocampal synaptic plasticity and memory in Huntington's disease, bioRxiv doi: 10.1101/297069.
64. Domanov YA, Aimon S, Toombes GE, Rennter M, Quemeneur F, Triller A, Turner MS, Bassereau P, Mobility in geometrically confined membranes, Proc. Natl. Acad. Sci. USA 108 (2011) 1260512610.
65. Pierobon P, Achouri S, Courty S, Dunn AR, Spudich JA, Dahan M, Capello G, Velocity, processivity, and individual steps of single myosin V molecules in live cells, Biophys. J 96 (2009) 42684275.
66. Groc L, Lafourcade M, Heine M, Renner M, Racine V, Sibarita JB, Lounis B, Choquet D, Cognet L, Surface trafficking of neurotransmitter receptor: comparison between single-molecule/quantum dot strategies, J. Neurosci 27 (2007) 12433–12437. [PubMed: 18003820]
67. Lee SH, Jin C, Cai E, Ge P, Ishitsuka Y, Teng KW, de Thomaz AA, Nall D, Baday M, Jeyifous O, Demonte D, Dundas CM, Park S, Delgado JY, Green WN, Selvin PR, Super-resolution imaging of synaptic and extra-synaptic AMPA receptors with different-sized fluorescent probes, Elife 6 (2017) e27744. [PubMed: 28749340]
68. Nechyporuk-Zloy V, Dieterich P, Oberleithner H, Stock C, Schwab A, Dynamics of single potassium channel proteins in the plasma membrane of migrating cells, Am. J. Physiol. Cell Physiol 294 (2008) C1096–1102. [PubMed: 18287336]
69. Howarth M, Liu W, Puthenveetil S, Zheng Y, Marshall LF, Schmidt MM, Wittrup KD, Bawendi MG, Ting AY, Monovalent, reduced-size quantum dots for imaging receptors on living cells, Nat. Methods 5 (2008) 397–399. [PubMed: 18425138]
70. Abraham L, Lu HY, Falcao RC, Scurll J, Jou T, Irwin B, Tafleh R, Gold MR, Coombs D, Limitations of Qdot labelling compared to directly-conjugated probes for single particle tracking of B cell receptor mobility, Sci. Rep 7 (2017) 11379. [PubMed: 28900238]
71. Wichner SM, Mann VR, Powers AS, Segal MA, Mir M, Bandaria JN, DeWitt MA, Darzacq X, Yildiz A, Cohen BE, Covalent protein labeling and improved single-molecule properties of aqueous CdSe/CdS quantum dots, ACS Nano 11 (2017) 6773–6781. [PubMed: 28618223]
72. Liu W, Howarth M, Greytak AB, Zheng Y, Nocera DG, Ting AY, Bawendi MG, Compact biocompatible quantum dots functionalized for cellular imaging, J. Am. Chem. Soc 130 (2008) 1274–1284. [PubMed: 18177042]
73. Lee J, Feng X, Chen O, Bawendi MG, Huang J, Stable, small, specific, low-valency quantum dots for single-molecule imaging, Nanoscale 10 (2018) 4406–4414. [PubMed: 29451567]
74. Farlow J, Seo D, Broaders KE, Taylor MJ, Gartner ZJ, Jun YW, Formation of targeted monovalent quantum dots by steric exclusion, Nat. Methods 10 (2013) 1203–1205. [PubMed: 24122039]
75. Nirmal M, O Dabbousi B, Bawendi MG, Macklin JJ, Trautman JK, Harris TD, Brus LE, Fluorescence intermittency in single cadmium selenide nanocrystals, Nature 383 (1996) 802–804.
76. Efros A. l., Nesbitt DJ, Origin and control of blinking in quantum dots, Nat. Nanotechnol 11 (2016) 661–671. [PubMed: 27485584]
77. Orfield NJ, McBride JR, Keene JD, Davis LM, Rosenthal SJ, Correlation of atomic structure and photoluminescence of the same quantum dot: pinpointing surface and internal defects that inhibit photoluminescence, ACS Nano 9 (2015) 831–839. [PubMed: 25526260]
78. Orfield NJ, McBride JR, Wang F, Buck MR, Keene JD, Reid KR, Htoon H, Hollingsworth JA, Rosenthal SJ, Quantum yield heterogeneity among single nonblinking quantum dots revealed by atomic structure-quantum optics correlation, ACS Nano 10 (2016) 1960–1968. [PubMed: 26849531]
79. Wang Y, Fruhwirth G, Cai E, Ng T, Selvin PR, 3D super-resolution imaging with blinking quantum dots, Nano Lett 13 (2013) 5233–5241. [PubMed: 24093439]
80. Grimm JB, English BP, Choi H, Muthusamy AK, Mehl BP, Dong P, Brown TA, LippincottSchwartz J, Liu Z, Lionnet T, Lavis LD, Bright photoactivatable fluorophores for single-molecule imaging, Nat. Methods 13 (2016) 985–988. [PubMed: 27776112]

81. Tsunoyama TA, Watanabe Y, Goto J, Naito K, Kasai RS, Suzuki KGN, Fujiwara TK, Kusumi A, Super-long single-molecule tracking reveals dynamic-anchorage-induced integrin function, Nat. Chem .Biol 14 (2018) 497–506. [PubMed: 29610485]

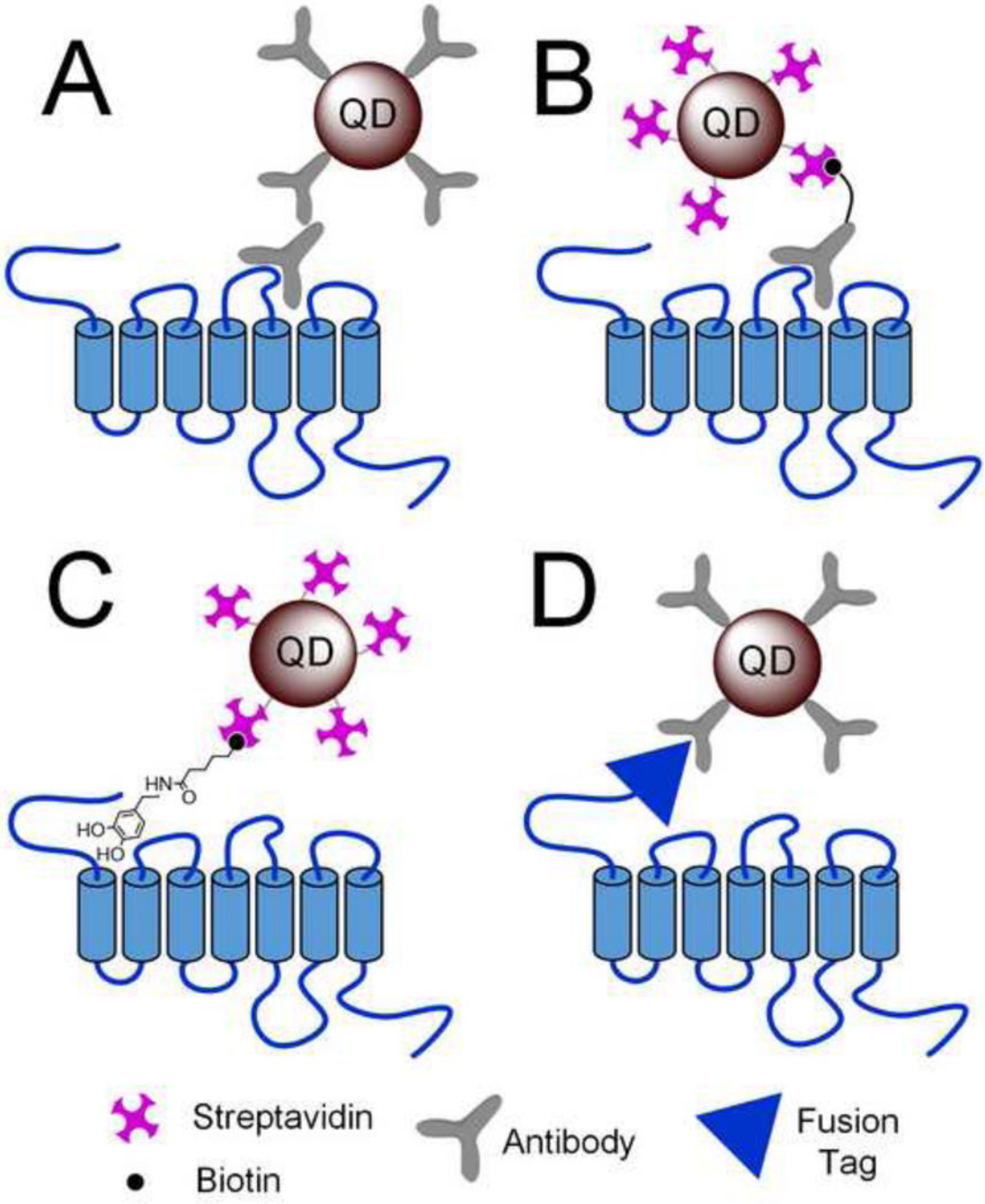

Figure 1.

A diagram depicting popular QD labeling strategies (not to scale). (A) The target molecule is first labeled with a primary antibody against its native extracellular epitope and then tagged with secondary antibody-conjugated QDs. (B) A biotinylated primary antibody is first used to label the target molecule, and its biotin terminus is subsequently captured by streptavidin-conjugated QDs. (C) Our strategy relies on the use of high-affinity biotinylated organic ligands that bind to the target molecule and are subsequently captured by streptavidin-conjugated QDs. (D) In the absence of a suitable extracellular epitope, an

appropriate fusion tag can be genetically introduced at one of the extracellular termini or into the extracellular loop and subsequently be tagged with QDs.

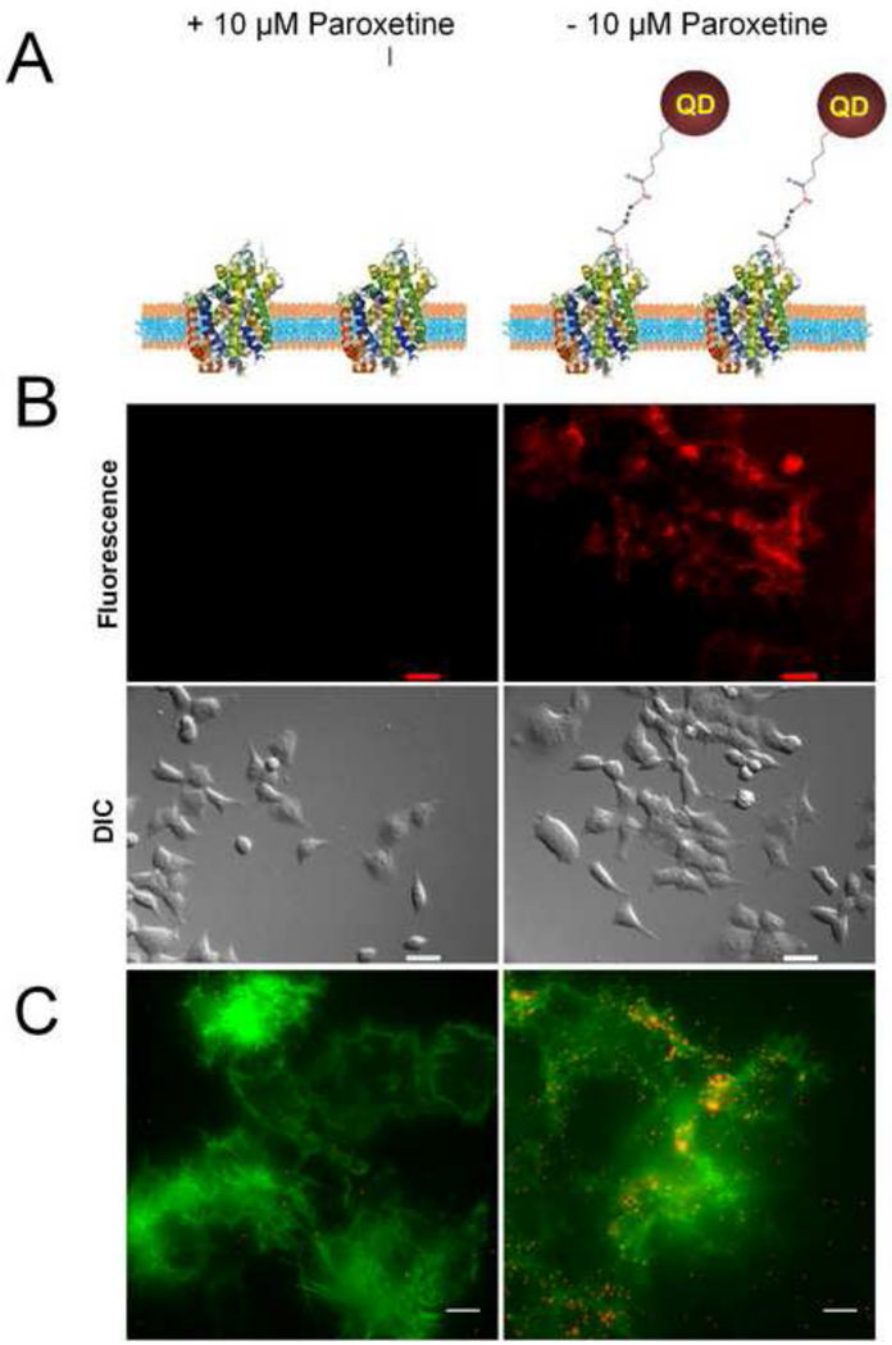

Figure 2.

Schematic of a Qdot-based fluorescence assay for evaluating binding affinities of SERT-specific, biotinylated, PEGylated ligands. (A) In a two-step protocol, SERT-expressing HEK293T cells grown in 24-well plates were labeled with a biotinylated ligand (500 nM for 10 min) and streptavidin-conjugated Qdots (1 nM for 5 min). To assess nonspecific binding, parallel wells were preincubated with paroxetine, a high-affinity SERT inhibitor with K_i = 0.6 nM (10 μM for 10 min). (B) Representative widefield fluorescence and DIC images demonstrating specific labeling of SERT-expressing HEK293T cells with 500 nM IDT357

and 1 nM QD655 (9). Scale bar: 40 μm. (C) Representative widefield fluorescence images demonstrating specific labeling of YFP-SERT-expressing HEK293 cells with 500 nM IDT357 and 20 pM QD655. Scale bar: 10 μm.

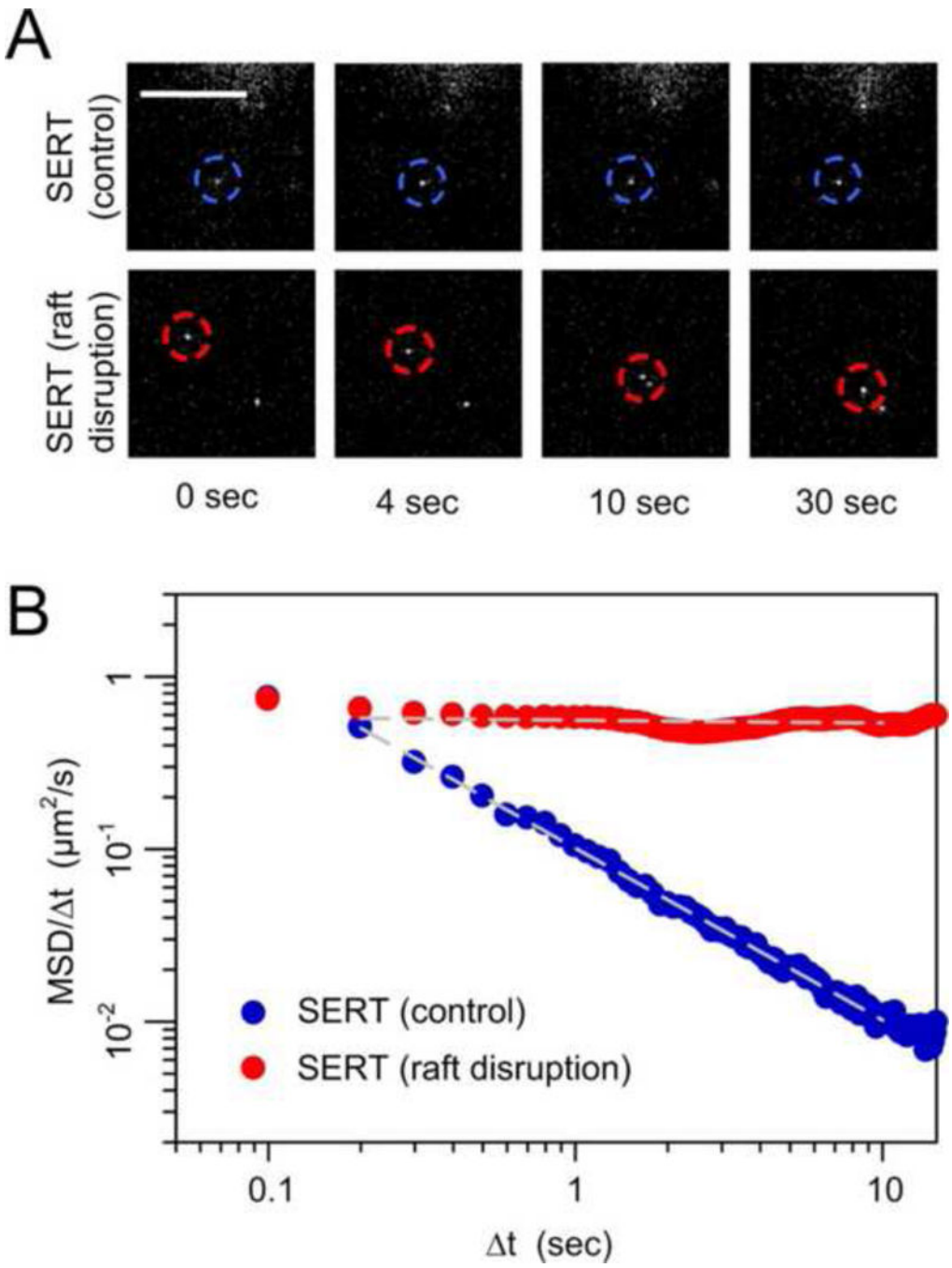

Figure 3.

Single QDot tracking of a SERT in living serotonergic RN46A cells under control and lipid raft-disrupted conditions. (A) Temporal profile of representative QDot-labeled, single SERTs with and without lipid raft disruption. Note the more mobile behavior of the single QDot after lipid raft disruption. The scale bar is 10 μm. (B) Comparison of the mean-squared displacement over time of the representative single QDots in (A). A single SERT under a lipid raft-disrupted condition shows the pattern expected of free diffusion, whereas a

single SERT from untreated cells demonstrates a pattern consistent with confined lateral diffusion. Reproduced with permission from [25].

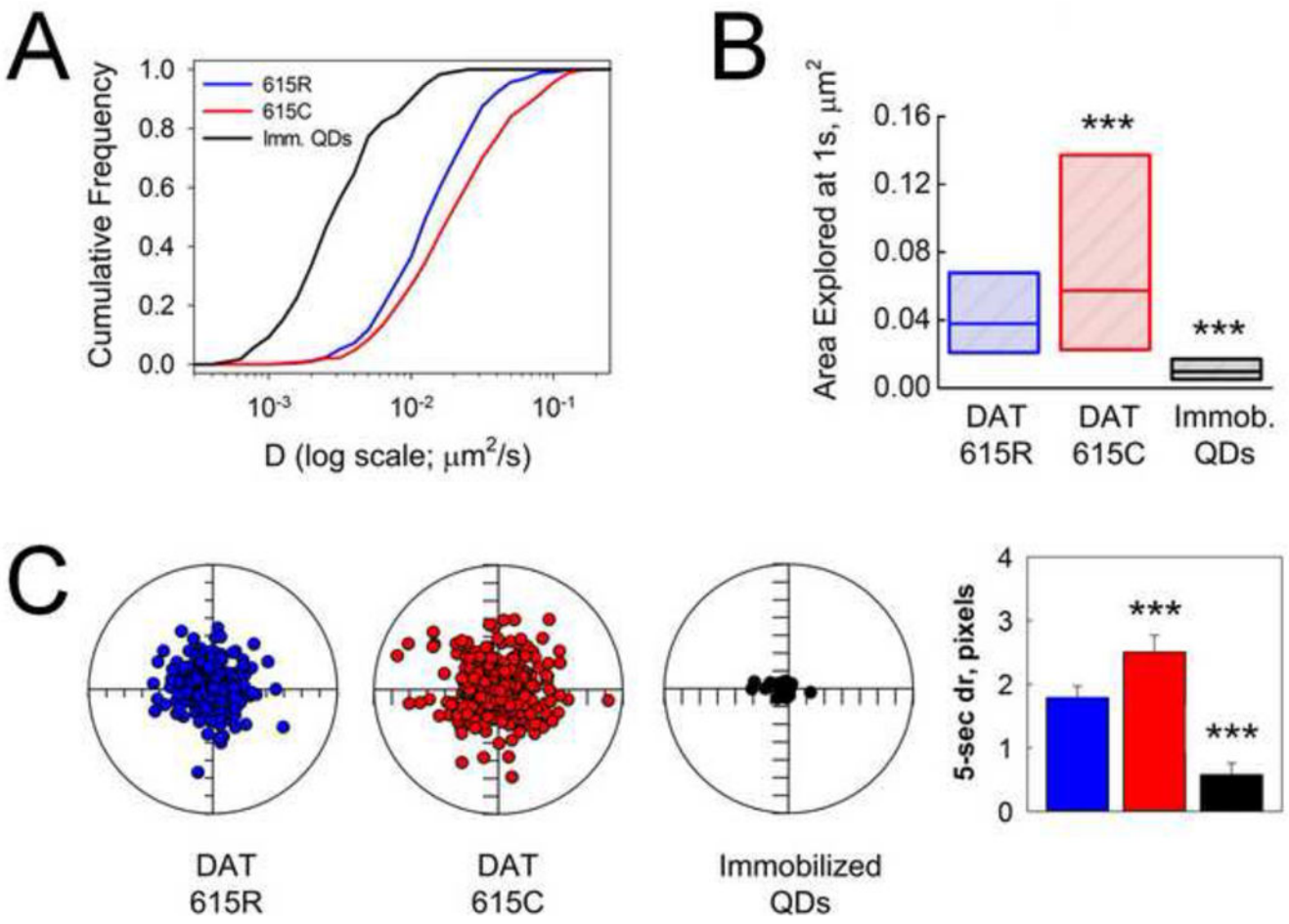

Figure 4.

Single quantum dot tracking of the wildtype DAT 615R variant and the ADHD-derived DAT 615C variant. (A) Cumulative probability plots depicting diffusion rate distributions (one-way ANOVA with Bonferroni-Dunn's post hoc test on raw diffusion coefficient values: DAT 615R vs DAT 615C, ***P < 0.001; DAT615R vs immobilized QDs on a coverslip, ***P < 0.001). (B) Explored areas at 1 s, shown as color box plot histograms. Median is represented as a line; color box represents the 25%–75% interquartile range (one-way ANOVA with Bonferroni-Dunn's post hoc test: DAT 615R vs DAT 615C, ***P < 0.001; DAT615R vs Immobilized QDs on a coverslip, ***P < 0.001). (C) Two-dimensional polar plots of 5 s radial displacements (d_{5s}) of single QD-DAT 615R, QD-DAT 615C, and immobilized QDs normalized to their starting coordinates. Radius of a polar plot is 2.8 μm. Pixel size is 200 nm. Mean d_5 values were compared using one-way ANOVA with Bonferroni-Dunn's post hoc test; ***P < 0.001 with respect to QD-DAT 615R. Asterisks in B and C denote P < 0.001 statistical significance level. Reproduced with permission from [27].

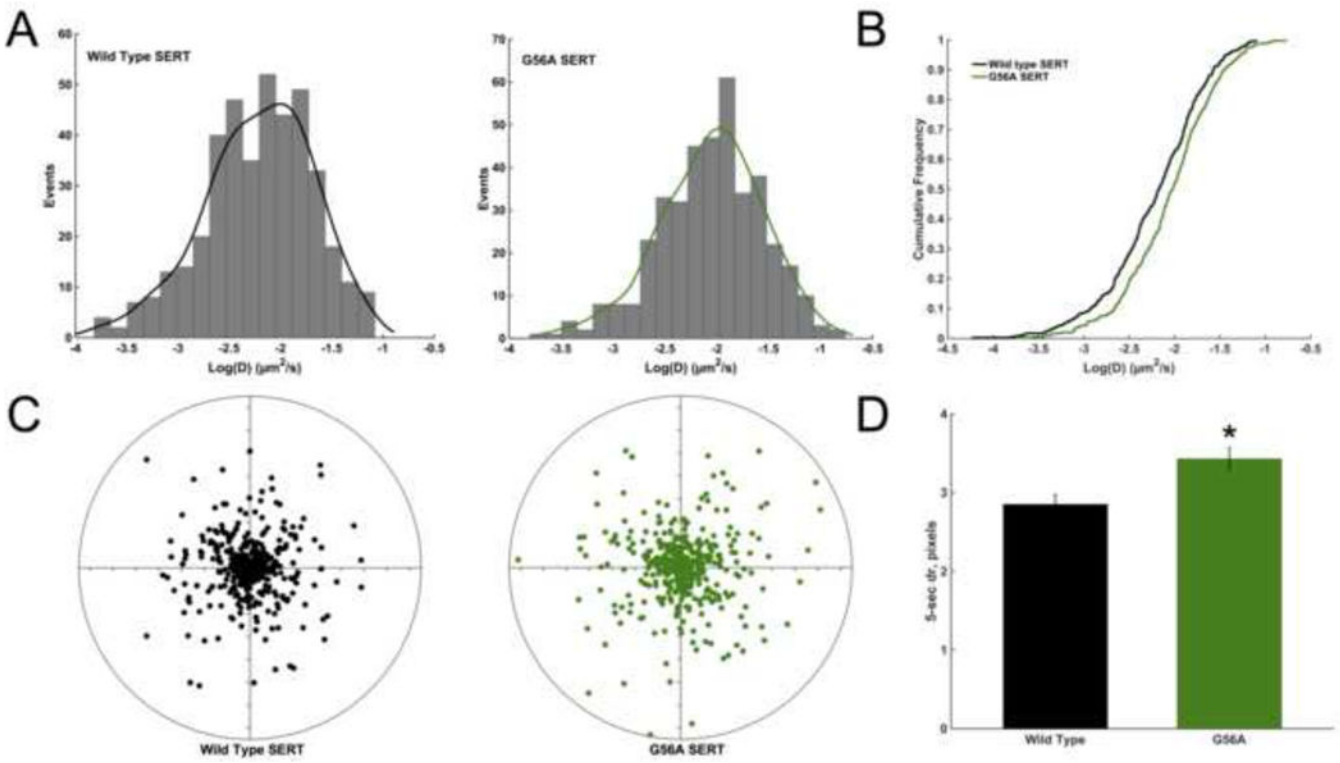

Figure 5.

Single QD tracking revealed differences in lateral mobility and diffusion between wild type SERT and autism-associated G56A SERT in stably transfected CHO cells (n>400 trajectories per condition from at least three independent experiments). (A) Distributions of diffusion coefficients for wild type SERT and G56A SERT. (B) Cumulative probability plots portraying diffusion coefficient distributions for both conditions; ***p<0.001, Kolmogorov-Smirnov test. (C) Two-dimensional polar plots of five second displacements of single SERT proteins normalized to starting positions for wild type SERT and G56A SERT. Radius of a polar plot is 1.3 μm. (D) Wild type SERT and G56A SERT mean radial displacement values (magnitude of 5-sec vector displacement from the origin); pixel size is 108 nm; *p<0.01, Student's t-test.

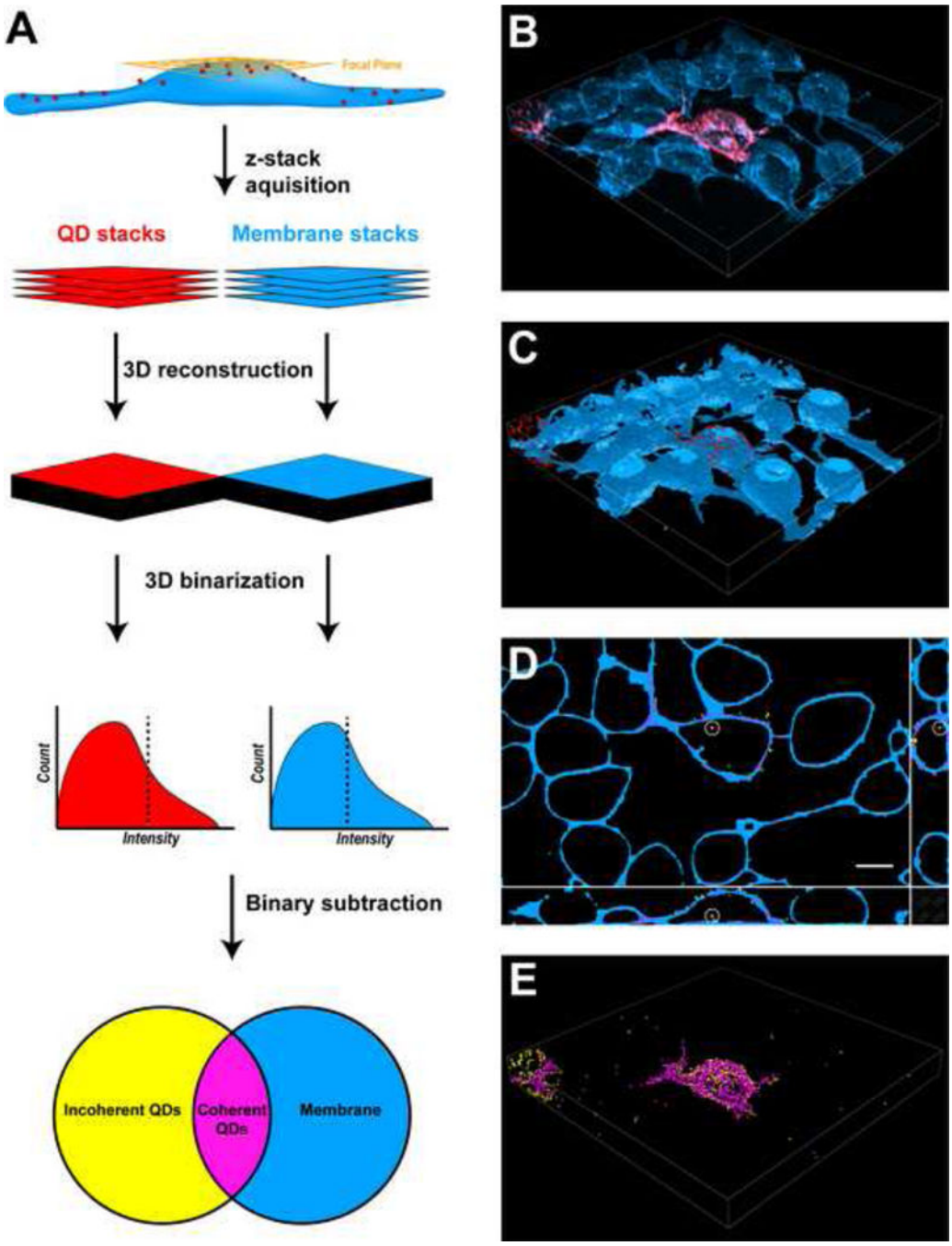

Figure 6.

Spinning-disk confocal microscopy and single QD localization to analyze endocytosed DAT. (A) An analytical workflow outlining image z-stack acquisition, 3D reconstruction, 2channel 3D binarization, and subtractive object analysis. Note the Venn diagram demonstrates discrimination of QD object coherence to the cell membrane localization. (B) A representative 3D image overlay of an HEK293 cell expressing DAT labeled with ligand-conjugated QDs (red) and cell membranes labeled with CellMask (blue). (C) 3D binarized imaging data represented in (B) of both QD and CellMask channels. (D) A Z-slice

accompanied by orthogonal XZ and YZ slices highlighting membranous (magenta) and nonmembranous (yellow) DAT-QDs. The endocytosed DAT-QD is clearly demonstrated (white circles). (E) A 3D representation of the binarized QD channel in [C] nonmembranous and membranous DAT-QDs.

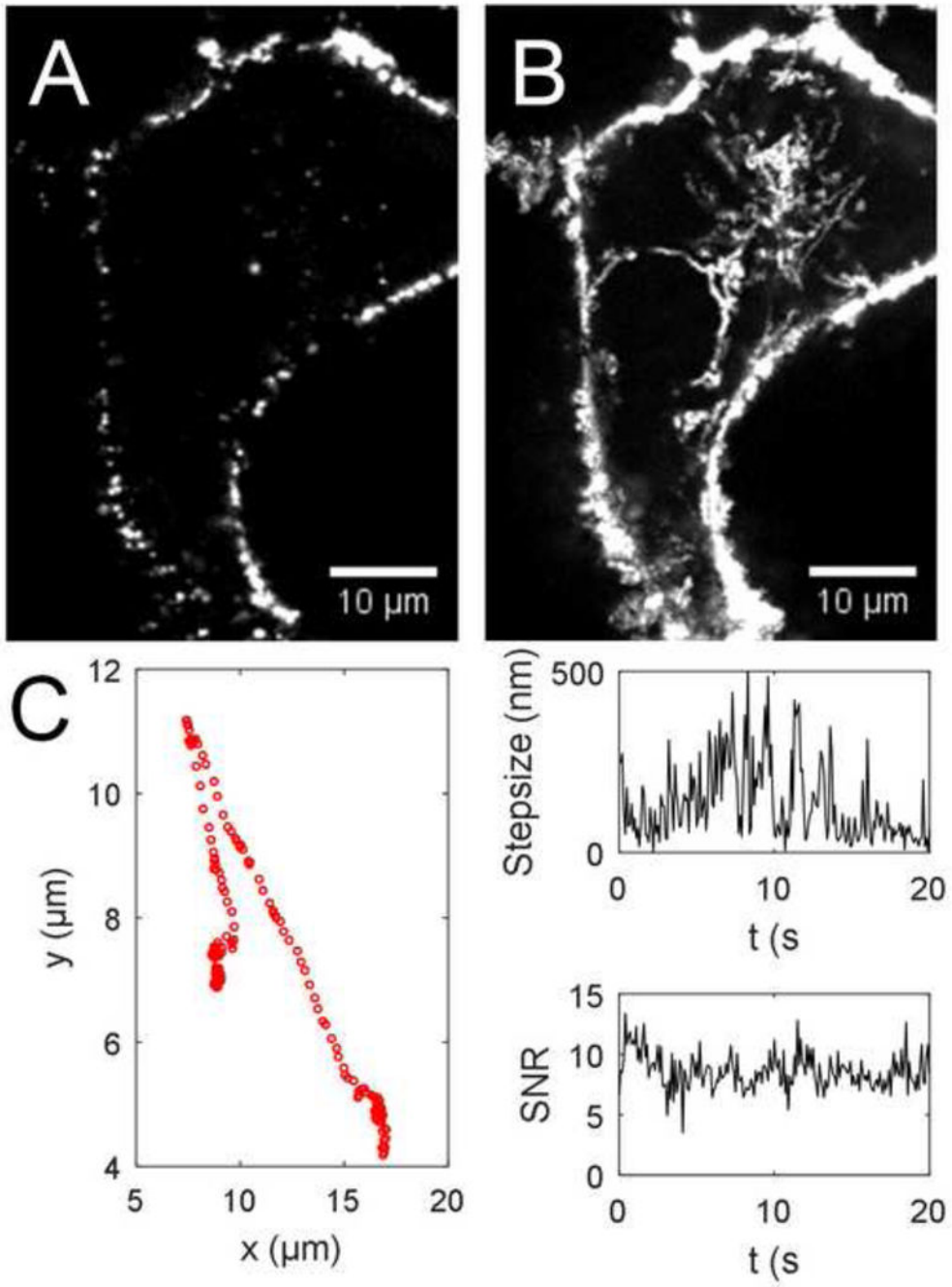

Figure 7.

Tracking single endocytosed DAT-QDs. (A) A fluorescence image of a cross-section of a DAT-expressing HEK293 cell labeled with ligand-conjugated QDs. DAT-QDs were allowed to constitutively internalize during one-hour incubation on the heated stage of the spinning-disk confocal microscope. (B) A maximum intensity projection of a time-lapse stack of the cell region shown in (A) acquired at 10 Hz for 1 min. Intracellular DAT-QD tracks are readily apparent. (C) An example trajectory of a DAT-QD complex being actively

transported inside the cell. High SNR allows accurate determination of the active transport dynamic parameters, such as instantaneous displacement or step size.

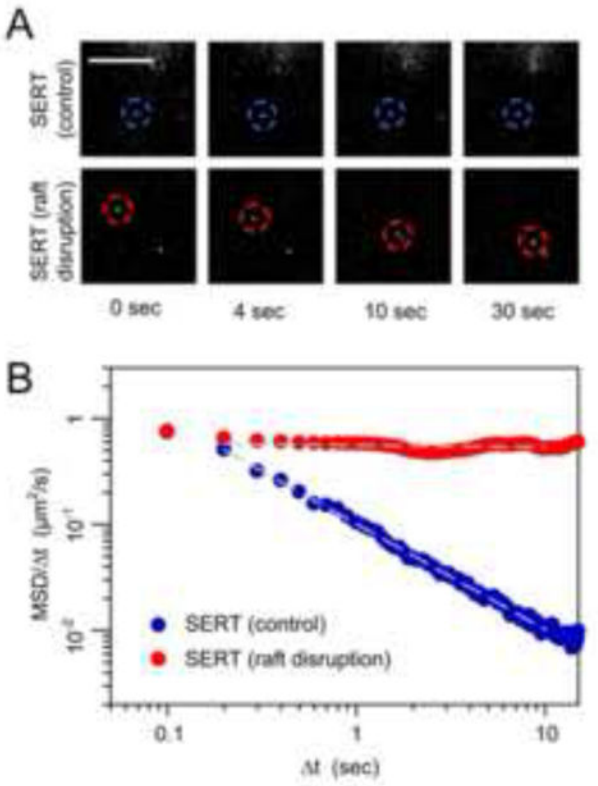

Scheme 1.

Synthesis of the biotinylated, PEGylated homotryptamine derivative IDT357 used in this study. (i) acetonitrile, triethylamine, reflux 18 hours; (ii) (a) ethanol, hydrazine mono hydrate, ambient temperature, 1 hour. (b) CH_2Cl_2, ambient temperature, 18 hours; (iii) CH_2Cl_2, ambient temperature, 18 hours.

Table 1.

A list of several single quantum dot tracking evolution milestones. Quantum dot milestones in the field of neuroscience are highlighted in light grey.

Single Quantum Dot Tracking Evolution Milestones	Research Group	Year	Reference
Introduction of QDs to biological imaging	Marcel Bruchez, A. Paul Alivisatos, Shuming Nie	1998	4, 5
Ultrahigh-resolution multicolor colocalization of single QDs	Shimon Weiss	2000	50
First report of ligand-conjugated QDs targeting a neuronal membrane protein	Sandra Rosenthal	2002	23
First report of antibody- and streptavidin-conjugated QDs	Marcel Bruchez	2002	51
First report of QD use in SPT, tracking neuronal glycine receptors	Antoine Triller	2003	6
Simultaneous two-color QD tracking	Diane and Keith Lidke	2005	52
Intracellular QD tracking (kinesin motors)	Maxime Dahan	2006	53
Structural basis for near unity quantum yield in QDs revealed	James McBride and Sandra Rosenthal	2006	54
Astigmatic lens-assisted 3D QD tracking	Thomas Schmidt	2007	12
3D QD tracking with multifocal plane \microscopy	Raimund Ober	2008	14
First report of QD use in presynaptic vesicle tracking	Richard Tsien	2009	55
3D QD tracking using a double-helix point spread function	W. E. Moerner	2010	13
First report of single quantum dot tracking of a monoamine neurotransmitter transporter (SERT)	Sandra Rosenthal	2011	25
Spectral blueing and blinking-assisted QD superresolution imaging	Stefan Hell	2011	56
High-speed (up to 1.75 kHz) QD tracking	B. Christoffer Lagerholm	2013	15
Hyperspectral eight-color QD tracking	Diane and Keith Lidke	2013	9
First report of QD tracking of a membrane protein in organotypic brain slices	Jean-Baptiste Sibarita and Martin Heine	2014	10
Astigmatism-assisted 3D QD tracking in brain slices	Martin Heine	2015	57
QD-based stimulated emission by depletion (STED) superresolution imaging	Stefan Hell	2015	58
QD tracking of D1 dopamine receptors in acute brain slices	Laurent Groc	2016	11

Table 2.

Destabilization of surface diffusion dynamics of membrane proteins in human disorders.

Genetic Cause	Molecular Phenotype	Disorder	Reference
Mutated stargazin, a protein responsible for synaptic accumulation of α-amino-3-hydroxy-5-methyl-4-isoxazolepropionic acid (AMPA) receptors	increased AMPAR lateral mobility	absence epilepsy, cerebellar ataxia	59
Deletion of N-cofilin, a key regulator of synaptic actin turnover and dendritic spine shape/size	increased extrasynaptic AMPAR mobility	Associative Learning impairment	60
Delta-F508 mutation in the cystic fibrosis transmembrane conductance regulator (CFTR) chloride channel	delta-F508 CFTR diffusion more rapid than wildtype CFTR	cystic fibrosis	61
Copy number variation of the cytoplasmic FMRP-interacting protein 1 (CYFIP1), critical for maintenance of dendritic spine complexity and morphology	increased AMPAR mobility in synaptic clusters of CYFIP1deficient neurons	schizophrenia, autism spectrum disorder	62
Exon1 mutations in huntingtin, resulting in the polyglutamine expansion	increased AMPAR mobility	Huntington's disease	63
C-terminus R615C mutation in dopamine transporter (DAT)	DAT-R615C diffusion more rapid than wildtype DAT	attention deficit/hyperactivity disorder	27
N-terminus G56A mutation in serotonin transporter (SERT)	SERT-G56A diffusion more rapid than wildtype SERT	autism spectrum disorder	Here in Section 3.3
*Serum autoantibodies against N-methyl-D-aspartate glutamate receptors (NMDAR)	increased NMDAR mobility and synaptic exchange rate	schizophrenia, psychosis	46

Asterisk denotes a non-genetic underlying cause of the disorder.